In-Building DAS for High Data Rate Indoor Mobile Communication

Temitope Alade, Hassan Osman and Miranda Ndula
University of Kent, Canterbury, United Kingdom

***Abstract*—As well known, providing high data rate wireless mobile services is difficult in indoor environments, particularly in multi-floor buildings. One way to achieve high data rate wireless transmissions is to reduce the radio transmission distance between the transmitter and the receiver by using distributed antenna systems (DASs) employing frequency reuse. However, frequency reuse causes co-channel interference, which is detrimental to system performance. In this paper, the impact of co-channel interference on the achievable uplink spectral efficiency of an in-building wireless communication system employing DAS is examined. In the system, remote antenna units (RAUs) are deployed on each floor throughout the building and connected to a central unit (CU) where received signals are processed. System performance is investigated by using a propagation channel model derived from multi-floor, in-building measurement results. The proposed scheme exploits the penetration loss of the signal through the floors, resulting in frequency reuse in spatially separated floors, which increases system spectral efficiency and also reduces co-channel interference. Location based RAU selection and deployment options are investigated. System performance is evaluated in terms of location-specific spectral efficiency for a range of potential mobile terminal (MT) locations and various in-building propagation characteristics.**

***Index Terms*—Distributed antenna system (DAS), Co-channel interference, Multi-floor in-building propagation, Spectral efficiency.**

I. Introduction

Due to the advent of smart phones, ipads and various handheld units, there has been increasing demands for high data rate multimedia services particularly for mobile terminals (MTs) operating within buildings. In such environments, delivering high quality in-building wireless services with the existing macrocell system remains a major challenge due to long radio transmission distance, limited bandwidth and electromagnetic shielding of wireless signals by floors and walls inside the building [1].

To enhance data rates and improve wireless coverage with limited bandwidth and low transmit power, different techniques are widely used, and distributed antenna system (DASs), which employ multiple remote antenna units (RAUs) connected to a home base station (or central unit) have drawn considerable attention in recent years, due to its enormous improvement in terms of better coverage, and higher data rates [2]. RAUs in DAS are geographically distributed so that the radio transmission distance from a MT to the surrounding RAUs is reduced and a high signal-to-noise ratio (SNR) is guaranteed.

However, most of the recent work on the conventional DAS have been focused on outdoor environments with cell sizes generally within thousands of meters. In [3], it has been shown that DAS reduces co-channel interference in a multicell environment, and hence significantly improves system performance and capacity, particularly for MTs near cell boundaries. However, the research results published cannot be applied directly to three-dimensional (3D) in-building multi-floor propagation environments. This is mainly because, buildings represent challenging environments, complicated by the large variability in building layout, architectural styles, and building materials. The paths generated by reflection and transmission within the building may increase the level of co-channel interference, which may greatly diminish the advantages of DAS, if the same frequency channels are reused in adjacent floors of high-rise buildings [4]. Thus, to analyse and design multi-floor in-building wireless systems, it is necessary to explore the characteristics of the indoor propagation channel and develop a propagation channel model, which accounts for inter-floor interference caused by the building structure and its terrain. This exploration is also important when deploying indoor femtocell system which is one of the technologies planned for future in-building mobile communication systems [5].

The mechanisms governing indoor radio propagation have been studied through experimental measurements and raytracing techniques. Rappaport et al. [6] presented site specific models which included measured path loss due to obstructions such as walls, soft partitions and floors. Furthermore, [7] used ray-tracing techniques to predict in-building propagation characteristics with reasonable accuracy. This paper explores the performance of DAS for high data rate indoor users in the presence of co-channel interference. Radio channel propagation characteristics in indoor high-rise buildings, with frequency reuse among floors, and the resulting impact on system performance are examined. The achievable spectral efficiency is used as the metrics to measure the performance of the wireless system.

II. PROPAGATION AND CHANNEL MODEL

A. *Propagation model*

The uplink transmission model in a multi-storey building is shown in Fig. 1, where each storey is treated as a cell with the floors forming natural boundaries. Multiple ceiling mounted RAUs are evenly located in the same position on every floor, to serve all MTs on each floor. The RAUs in their turn, are connected to a central unit (CU) where received signals are constructively processed. Each floor of the building has a similar construction with an open office interior floor plan and the same frequencies are assumed to be reused on each floor. However, frequency reuse within the same floor is avoided in order to reduce interference, which implies that co-channel interference can only emanate from co-channel MTs from nearby floors.

978-1-4673-0990-5/12/$31.00 ©2012 IEEE

In the building, it is assumed there are a total of U CUs, one on each floor and each CU consist of N RAUs. For simple analysis, it is assumed that the floors are shaped as cubes with a common inter-floor spacing of F meters and there is one active MT evenly located across each floor at height of v meters; however, this investigation can be extended to multiple MTs per floor. The MT of interest $u^{'}$ is located on the middle floor (reference floor) of the building. It is also assumed that there is a multistorey building located a few meters away from the reference building.

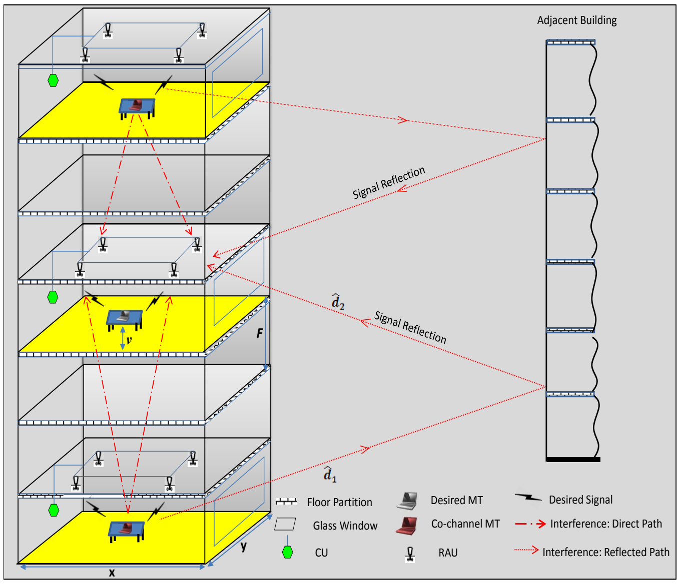

Fig. 1. In-Building DAS with frequency reuse in every floor

In radio propagation between floors of high-rise buildings, experimental results have shown that there are two possible sources of interference. Depending on the structure of the building, the location of the transmitter and the receiver, co-channel inference could emanate from [8]

1) direct signal transmission through the floor partitions, which may include multiple reflections between the walls, floors and ceilings;
2) transmissions that involve signal reflections and scattering from a nearby building that propagates back into the reference floor.

In uplink transmission of the DAS investigated in this paper, co-channel interference from the direct and the reflected paths is considered. In this case, a RAU will receive a desired signal from a MT, and interfering signals emanate from other MTs on co-channel floors via direct ray penetration through the floors and reflections from nearby buildings.

The transmitted signal from MT-u to the n-th RAU may be expressed as

$$x_u(t) = Re\left[\sqrt{P_s}\sum\nolimits_{i=-\infty}^{\infty} b_u\left[i\right]\rho_{T_s}(t-iT_s)e^{j2\pi f_c t}\right] \quad (1)$$

where $Re[x]$ represents the real part of x, P_s is the transmit power which is assumed to be the same for all MTs, $b_u\left[i\right]$ is the transmitted symbol, T_s represent the symbol duration, $E[b_u]=0$ and $E[b_u]^2=1$. $\rho_{T_s}(t)$ is a pulse waveform defined as $\rho_{T_s}(t)=1$ for $0\leq t\leq T_s$ and $\rho_{T_s}(t)=0$ otherwise and f_c is the carrier frequency.

B. Channel model

The channel from MT-u to the n-th RAU on the reference floor is modelled as the sum of low pass equivalent impulse responses of the individual paths which may be expressed as

$$h_{u,n}(t) = h^{'}_{u,n}(t) + \hat{h}_{u,n}(t) \quad (2)$$

where $h^{'}_{u,n}(t)$ and $\hat{h}_{u,n}(t)$ are the impulse responses for the paths that run through the floors and the reflected paths from surrounding building respectively. Details of the channel model have been reported in a previous paper [9].

Accordingly, the received signal by the n-th RAU on the reference floor includes components from the desired MT-$u^{'}$, co-channel interfering MT-u from other floors of the building and noise. This may be represented by its complex low-pass equivalent as

$$\begin{aligned} r_{u,n}(t) &= (d_{u^{'},n})^{-\lambda/2}\cdot\alpha_{u^{'},n}\cdot e^{j\theta_{u^{'},n}}\cdot x_{u^{'}}(t-\tau_{u^{'},n}) \\ &+ \sum_{u=1,u\neq u^{'}}^{U}(G_d+Q_r)\cdot x_u(t-\tau_{u,n})+\eta_n(t) \end{aligned} \quad (3)$$

where $G_d=(d_{u,n})^{-\lambda/2}\cdot\varphi^{k}_{u,n}\cdot\alpha_{u,n}\cdot e^{j\theta_{u,n}}$, $Q_r=(\hat{d}_{u,n})^{-\lambda/2}\cdot\hat{\varphi}^{1/2}_{u,n}\cdot\ddot{\varphi}_{u,n}\cdot\hat{\alpha}_{u,n}\cdot e^{j\hat{\theta}_{u,n}}$ and $\eta_n(t)$ is the complex-valued additive white Gaussian noise (AWGN) received by the n-th RAU, which has a zero mean and a double sided power spectral density $N_0/2$. The envelop of the desired signal is modelled by Nakagami-m distribution. Hence, $\alpha^2_{u^{'},n}$ is Gamma distributed with the probability distribution function (pdf) expressed as [10]

$$p_{\alpha^2_{u^{'},n}}(\alpha^2_{u^{'},n}) = (\frac{m_n}{\Omega_n})^{m_n}\frac{(\alpha^2_{u^{'},n})^{m_n-1}}{\Gamma(m_n)}\exp(-\frac{m_n}{\Omega_n}\alpha^2_{u^{'},n}), \quad \alpha_{u^{'},n}\geq 0 \quad (4)$$

where m_n is a parameter accounting for the fading severity and Ω_n is the average fading power of the received signal. The parameters Ω_n and m_n may be expressed as $\Omega_n=E[\alpha^2_{u^{'},n}]$ and $m_n=\frac{\Omega_n^2}{E[(\alpha^2_{u^{'},n}-\Omega_n)^2]}, m_n\geq\frac{1}{2}$ respectively. It is assumed that interfering signals from other floors of the building have no specular component; therefore, the envelop of the interfering signal is Rayleigh distributed with the mean square $E[\alpha^2_{u,n}]=1$. The pdf of the instantaneous interfering signal power in the Rayleigh fading channel can be obtained by letting $m_n=1$.

Assuming the phase and the path delay are known at the receiver and the receiver has a perfect timing synchronisation with the MT-$u^{'}$ i.e., $\tau_{u^{'},n}=0$, the demodulated signal of MT-$u^{'}$ over one symbol period T_s is given by

$$Z_n = Re\left\{\frac{1}{T_s}\int_0^{T_s} r_{un}(t)dt\right\} = S_n+\sum\nolimits_{u=1,u\neq u^{'}}^{U} I_{u,n}+\eta_n \quad (5)$$

where S_n is the desired signal component, $I_{u,n}$ is the interfering signal component received from other floors and η_n the noise. After collecting the received signals from all RAUs on the reference floor, the total desired signal power is written as

$$S=\sum_{n=1}^{N}S_n^2=\left(\sum_{n=1}^{N}[\sqrt{P_s}(d_{u^{'},n})^{-\lambda/2}(\alpha_{u^{'},n})]\right)^2 \quad (6)$$

The expectation of the total interference component received on the reference floor via the N RAUs is given by $E[I_u] = 0$ and the variance denoted by $\sigma^2_{I_u}$ may be written as

$$\sigma^2_{I_u} = \sum_{n=1}^{N} \frac{P_s}{3} \sum\nolimits_{u=1,u\neq u'}^{U} [(d_{u,n})^{-\lambda}\varphi^k_{u,n} + (\hat{d}_{u,n})^{-\lambda}\hat{\varphi}_{u,n}\ddot{\varphi}_{u,n}] \tag{7}$$

It is assumed that the sum of all interferers can be approximated as zero mean Gaussian distributed noise by invoking the central limit theorem (CLT) since the number of interfering source is sufficiently large and interfering sources are independent of each other [11].

At the receiver, the minimum mean-square error combining (MMSEC) is applied and the signal received by the *n*-th RAU is multiplied by a controllable weight. Using MMSEC, the decision variable for detecting the desired signal may be expressed as

$$Z_0 = W^T Z_n = \sum_{n=1}^{N} [W_n] S_n + [W_n] I_{u,n} + [W_n]\eta_n \tag{8}$$

where W_n is the optimum weight vector which maximizes the SINR. Thus, the instantaneous SINR may be written as

$$\gamma = \sum_{n=1}^{N} \gamma_n = \frac{\left(\sum_{n=1}^{N} W_n S_n\right)^2}{\sum_{n=1}^{N} W_n^2 \sigma^2_{I_u} + \sum_{n=1}^{N} W_n^2 \sigma^2_{\eta}} = \sum_{n=1}^{N} \frac{A_n^2}{\rho_n} \alpha^2_{u',n} \tag{9}$$

where γ_n is the SINR per branch, $A_n^2 = P_s(d_{u',n})^{-\lambda}$ and $\rho_n = \frac{P_s}{3}\sum_{u=1,u\neq u'}^{U}\left[(d_{u,n})^{-\lambda}\varphi^k_{u,n} + (\hat{d}_{u,n})^{-\lambda}\hat{\varphi}_{u,n}\ddot{\varphi}_{u,n}\right] + \sigma^2_{\eta}$. The average SINR can be expressed as

$$\bar{\gamma} = \sum_{n=1}^{N} \frac{\frac{2E_s}{N_0} \cdot (d_{u',n})^{-\lambda}}{\frac{2}{3} \cdot \frac{E_s}{N_0} \sum_{u=1,u\neq u'}^{U} [D_u + R_u] + 1} \cdot \Omega_n \tag{10}$$

where $D_u = (\hat{d}_{u,n})^{-\lambda}\varphi^k_{u,n}$ and $R_u = (\hat{d}_{u,n})^{-\lambda}\hat{\varphi}_{u,n}\ddot{\varphi}^2_{u,n}$. $\frac{E_s}{N_0}$ is the transmit symbol energy-to -noise density ratio at the MT transmitter location, and E_s is expressed as

$$E_s = P_s \cdot T_s \tag{11}$$

The pdf of $\bar{\gamma}$ is obtained as [12]

$$P_{\gamma}(\gamma) = \frac{1}{\pi}\int_0^{\infty} \frac{cos\left[\sum_{n=1}^{N} m_n tan^{-1}\left(\frac{t}{\beta_n}\right) - t\gamma\right]}{\prod_{n=1}^{N}\left(1 + \left(\frac{t}{\beta_n}\right)^2\right)^{m_n/2}} \tag{12}$$

where $\beta_n = m_n/\bar{\gamma}_n$

III. Achievable Spectral Efficiency

The adaptive MQAM modulation which dynamically determines the modulation level based on the effective SINR is applied to maximize spectral efficiency while keeping the BER under a target level. This is essential since most applications require a certain maximum BER. During good propagation conditions, a higher order modulation scheme is used, while during a signal fade, the system selects a lower order modulation. The relationship between BER and SINR γ under a certain modulation order $M_j = 2^j$ for QAM can be approximated as [13]

$$\hat{P}_e(\gamma) = \frac{1}{5}\exp\left[\frac{-3\gamma}{2(2^j - 1)}\right] \tag{13}$$

where j is the number of bits per symbol. Given a target instantaneous BER equal to $\hat{P}_0$, the region boundaries (or adaptive modulator switching thresholds) γ_j for switching across the modulation orders can be solved from (13) and may be expressed as

$$\gamma_j = -\frac{2}{3}\ln(5\hat{P}_0)(2^j - 1); j = 0, 2, 3, \cdots J \tag{14}$$

where J is the maximum number of bits per symbol. The average spectral efficiency with unit of bits per second per Hertz, is defined as the sum of the data rates, $\log_2(M_j) = j$, weighted by the probability that the *j*-th modulation constellation is assigned to MT-u'. This may be expressed as

$$T_u = \sum_{j=1}^{J} log_2(M_j) \int_{\gamma_j}^{\gamma_{j+1}} P_{\gamma}(\gamma) d\gamma \tag{15}$$

where the values of γ_j and γ_{j+1} are obtained respectively according to (14) for a given $\hat{P}_0$. Note that $\gamma_{J+1} = +\infty$. By substituting (12) into (15), interchanging the order of integration and simplifying trigonometric identities, T_u can rewritten as

$$T_u = \sum_{j=1}^{J} log_2(M_j) \times \frac{1}{\pi}\int_0^{\infty} -\frac{sin(B_1(t) - t\gamma_{j+1}) - sin(B_1(t) - t\gamma_j)}{tB_2(t)} dt \tag{16}$$

where $B_1 = \sum_{n=1}^{N} m_n tan^{-1}(\frac{t}{\beta_n})$ and $B_2 = \prod_{n=1}^{N}(1 + (\frac{t}{\beta_n})^2)^{m_n/2}$

IV. Adaptive Antenna Selection via Interference Avoidance

An interference avoidance strategy, where a subset of N' strongest RAUs out of N available RAUs is selected for combining, is investigated in this section.

Due to the range of geometric arrangements possible with MTs and RAUS in uplink transmission, the achievable spectral efficiency is found to depend not only on the proximity of the desired MT to its RAU, but also on the location of the co-channel MT within the building because the path loss of the interfering signal can be much smaller than that of the desired signal in some locations across the floor. This finding is significant in terms of finding the number of RAUs to be selected for combining from N diversity branches. Although an increase in spectral efficiency is expected with increasing number of RAUs, it is important to note that some RAUs would have insignificant contribution to the total received signal. This is either due to high transmission path loss or the effect of co-channel MTs getting very close to RAUs located on the reference floor, such that $d_{u,n} < d_{u',n}$. These RAUs could be discarded to avoid interference and to save considerable amount of the receiver's signal processing. In conventional 2D outdoor cellular DAS networks, the RAUs with the shortest distance to the MT would be selected for combining; however, selecting such RAUs in uplink transmission of 3-D inter-floor communication may not enhance the system performance if a co-channel MT is located on a floor directly above (or below) the selected RAU. Therefore, a selection strategy which determines the appropriate RAUs to select for combining based on specific location of MTs is suggested. This way, the receiver would only combine RAUs with significant SINRs at any location across the entire floor before taking detection decision. This insight is validated by simulation in Section V through Fig. 4, where the achievable spectral efficiency is shown as a function of the parameter SNR for different values of N' at specific locations of MTs.

V. Numerical Results

In this section, a range of results for illustrating the achievable spectral efficiency of the exemplified DAS in high buildings is presented. The analytic formulas derived in Sections II-IV are numerically evaluated for the 7-storey building structure shown in Fig.1. A summary of parameters used in evaluating the performance of the system is listed in Table I, unless specified otherwise.

Figs.2 and 3 show location-specific achievable spectral efficiency over a range of possible locations of the desired MT across the reference floor when the co-channel MT is located at the back-left and center of the co-channel floor respectively. It is observed that the performance varies significantly and is strongly dependent on the specific location of the desired and the co-channel MTs. The achievable spectral efficiency shows four peaks at the location of the 4 RAUs; however, when the desired and the co-channel MTs are aligned at a RAU location, the performance degrades at that location as shown in the figures. It is also important to note that the achievable spectral efficiency reduces as the co-channel MT moves closer to the right side (position (40, x_u)) of the floor. This is due to significant contribution from reflected paths through the window as the co-channel MT moves closer to the window. The worst-case spectral efficiency is observed when the desired MT and the co-channel MT are located at the window side. At this location, the distances between desired MT and the RAUs are no smaller than any other location across the floor. Furthermore, the distances between co-channel MTs and the adjacent building are shortest at this location. Based on the above analysis of location-specific spectral efficiency, resource allocation can then be done efficiently through intelligent channel reuse in a multi-user environment [14-22]. For example, a MT can be assigned the same channel if a co-channel MT is not vertically aligned at the same location on immediate adjacent floors of the building.

Fig.4 shows the achievable spectral efficiency as a function of SNR for different values of N' at specific locations of MTs. These results have been obtained by considering 4 RAUs and comparing the performance when the strongest RAUs are selected. The desired and co-channel MTs are located at the left side ④, center ⑤ and right side ⑥ of the floor respectively. It is seen from this figure that when the MTs are located on the left side of the floor, the system performance for $N^{'} = 4$, $N^{'} = 3$ and $N^{'} = 2$ is very close. At this location, selecting two RAUs for combining, out of the 4 RAUs, achieve a spectral efficiency that is almost at optimal level. However, when MTs are located at the center of the floor, all RAUs should be selected. A similar performance behaviour to the left side is observed at the right side of the floor, where the 3 strongest RAUs are the useful diversity branches that can appreciably contribute to the received signal without any redundancy. The fourth RAU could be discarded due to strong co-channel interference. The discarded RAU represents no loss in appreciable received signal. This way, the requirement for phase and amplitude estimation on each RAU can be reduced.

VI. Conclusion

This study has shown that in-building DAS can improve data rates for indoor MTs. By considering co-channel interference emanating from vertically located MTs, the performance of the system is analytically quantified in terms of location specific spectral efficiency for a 7-storey building, by using a propagation channel model derived from multi-floor, in-building measurement data. The following conclusions have been drawn:

1) The highest spectral efficiency values are found in floor regions closer to the desired RAU, if a co-channel MT is not vertically aligned above the RAU location, while regions directly above/below the interfering MTs are found to have the lowest spectral efficiency values compared to rest of the floor. The worst case spectral efficiency occurs when the desired MT and the co-channel MT are both located close to the window.
2) By limiting the number of RAUs that are selected for combining, based on maximum received instantaneous power, which also reduces the effect of co-channel interference, RAUs with weak signal can be eliminated. The discarded RAUs represent no loss in appreciable spectral efficiency.

The proposed system is suitable for supporting a much higher number of MTs on the same frequency and high data rates can be achieved for indoor MTs.

TABLE I
Summary of Parameters

Parameters	Value
Number of floors in the building, U	7
Inter-floor spacing, F	4m
Floor dimension, (x, y)	40m X 40m
MT located across the floor at height, v	1m
Number of RAUs on each floor, N	4
Path loss exponent, λ	2.5
Penetration loss, φ	13dB
Reflection loss, $\hat{\varphi}$	8dB
Transmission coefficient through a glass window, $\ddot{\varphi}$	0.13dB
Nakagami fading value, m	$1.8, 1.5, 1.25, 1.0$
Distance between the reference and the adjacent building, $\hat{d}_{u,n}$	10m
Transmit SNR, E_s/N_0	30dB
Target BER, $\hat{P}_0$	10^{-3}dB

References

[1] H. Claussen, L. T. W. Ho, and L. G Samuel; An overview of the femtocell concept", *Bell Labs Tech.* J., 13:1 (2008), 221 - 245.

[2] Huiling Zhu, "Performance Comparison between Distributed Antenna and Microcellular Systems," *IEEE Journal on Selected Areas in Communications*, vol. 29, no. 6, pp. 1151-1163, June 2011

[3] X. You et al., "Cell edge performance of cellular mobile systems," *IEEE J. Select Areas Commun*, vol. 29, no. 6, pp. 1139-1150, June 2011.

[4] W. Honcharenko, H. L. Bertoni and J. Dailing,"Mechanism governing propagation between different floors in buildings"; *IEEE Trans. Antennas Propagation*, vol. 41. no. 6, pp 787-790 June 1993.

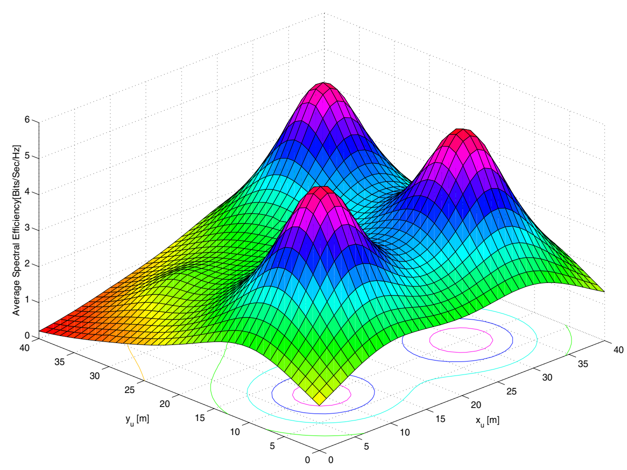

Fig. 2. Location-specific spectral efficiency (co-channel MT located at the back-left side of the floor)

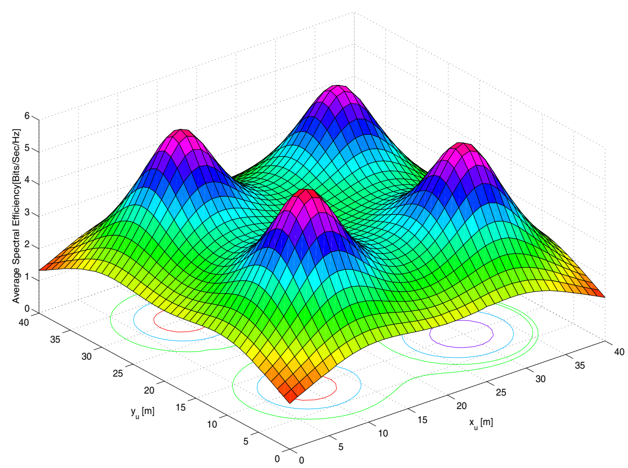

Fig. 3. Location-specific spectral efficiency (co-channel MT located at the floor center)

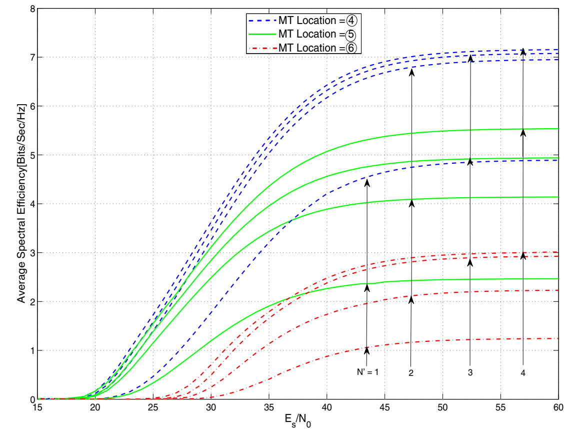

Fig. 4. Achievable spectral efficiency at specific MT locations when the strongest RAUs are selected

[5] Vikram Chandrasekhar et al., "Femtocell Networks: a Survey", *IEEE Communications Magazine*, vol. 46, no. 9 pp. 59-67, September 2008.

[6] M. A. Panjwani, A. L. Abbott, and T. S. Rappaport, "Interactive computation of coverage regions for wireless communication in multifloored indoor environments," *IEEE J. Select. Areas Commun.*, vol. 14, pp.420-430, Apr. 1996.

[7] R. A. Valenzuela, "A ray tracing approach to predicting indoor wireless transmission," in *proc. 43rd IEEE Veh.. Technol. Conf.*, 1993, pp. 214-218.

[8] Andrew C. M. Austin, Michael J. Neve, Gerard B. Rowe and Ryan J. Pirkl, "Modelling the effects of nearby buildings on inter-floor radio wave propagation"; *IEEE Trans. Antennas Propagation.*, vol. 57. no. 7, pp. 2155-2161 July 2009

[9] T. Alade H. Zhu and H. Osman, "Spectral Efficiency Analysis of Distributed Antenna Systems for In-Building Mobile Communication," *proc. IEEE GLOBECOM* 2011.

[10] J. Wang and J. Chen, "Performance of wideband CDMA with complex spreading and imperfect channel estimation," *IEEE Journal on Selected Areas in Communications*, vol. 19, no. 1, pp. 152-163, Jan. 2001.

[11] J. Wang and L. B. Milstein, "CDMA overlay situations for microcellular mobile communications," *IEEE Transactions on Communications*, vol. 43, no. 2/3/4, pp. 603-614, Feb/March/April 1995.

[12] G. Efthymoglou and V. Aalo, "Performance of RAKE receivers in Nakagami fading channel with arbitrary fading parameters"; *IEEE Electronic Letters*, Vol.31, No.18, pp. 1610-1612, Aug. 1995.

[13] M. S. Alouini and A. J. Goldsmith, "Adaptive modulation over Nakagami fading channels," *Wireless Pers. Commun.*, vol. 13, pp. 119-143, May 2000.

[14] H. Zhu and J. Wang, "Chunk-based resource allocation in OFDMA systems - Part I: chunk allocation," *IEEE Transactions on Communications*, vol. 57, pp. 2734-2744, no. 9, Sept. 2009.

[15] J. Chen, J. Wang and M. Sawahashi, "MCI cancellation for multicode wideband CDMA systems," *IEEE Journal on Selected Areas in Communications*, vol. 20, no. 2, pp. 450-462, Feb. 2002.

[16] B. Xia and J. Wang, "Effect of channel estimation error on QAM systems with antenna diversity," *IEEE Transactions on Communications*, vol. 53, no. 3, pp. 481-488, March 2005.

[17] Y. Q. Zhou, J. Wang and M. Sawahashi, "Downlink transmission of broadband OFCDM systems Part I: hybrid detection," *IEEE Transactions on Communications*, vol. 53, no. 4, pp. 718-729, April 2005.

[18] X. Y. Wang and J. Wang, "Effect of imperfect channel estimation on transmit diversity in CDMA systems," *IEEE Transactions on Vehicular Technology*, vol. 53, no. 5, pp. 1400-1412, Sept. 2004.

[19] H. Zhu and J. Wang, "Chunk-based resource allocation in OFDMA systems - Part II: joint chunk, power and bit allocation," *IEEE Transactions on Communications*, vol. 60, no. 2, February 2012.

[20] H. Zhu, B. Xia and Z. Tan, "Performance Analysis of Alamouti Transmit Diversity with QAM in Imperfect Channel Estimation," *IEEE Journal on Selected Areas in Communications*, vol. 29, pp. 1242-1248, no. 6, 2011.

[21] J. Wang, H. Zhu, and N. Gomes, "Distributed antenna systems for mobile communications in high speed trains," *IEEE Journal on Selected Areas in Communications*, vol. 30, 2012.

[22] H. Zhu, "Radio Resource Allocation for OFDMA Systems in High Speed Environments," *IEEE Journal on Selected Areas in Communications*, vol. 30, 2012.